Anthracenoyl Crown Ethers and Cryptands as Fluorescent Probes for Solid-Phase Transitions of Phosphatidylcholines: Syntheses and Phospholipid Membrane Studies†

Uwe Herrmann, Burkhard Tümmler,* Günter Maass, Philippe Koo Tze Mew, and Fritz Vögtle

ABSTRACT: Three structurally related crown compounds and cryptands have been synthesized that differ by the number and linkage of coronand units and anthracene moieties. The interaction of the fluorescent dyes with sonicated dimyristoylphosphatidylcholine (DMPC) vesicles is characterized by the relative quantum yields, uptake kinetics, binding curves, lifetimes, fluorescence titrations with water- and lipid-soluble quenching agents, fluorescence anisotropy, and equilibrium cooling curves. The most lipophilic compound II, which displays a similar quantum yield as the parent fluorophore 9,10-dimethylanthracene, shows a nearly equal distribution between solid and fluid lipid and is located at the bilayer surface. The least lipophilic compound IV is excluded from the hydrocarbon phase. The anthracenophane cryptand III preferentially partitions into solid-phase lecithins with the highest affinity for the phases L_ϵ and L_β. The binding constant to DMPC amounts to $(5.4 \pm 1.3) \times 10^2$ M^{-1} at 0 °C. From fluorescence quenching titrations it is concluded that the average position of the anthracenoyl dye III discontinuously shifts during the gel to liquid crystalline transition from the glycerol backbone to the choline head group. Electron microscopy and NMR experiments revealed that the anthracenophane induces in the liquid crystalline phase the fusion of small unilamellar DMPC vesicles to unilamellar medium-sized vesicles and macrovesicles, which subsequently fuse at the transition temperature to large multilamellar coacervates. Due to its large change of fluorescence intensity, the anthracenophane cryptand is a very sensitive probe for the detection of the pretransition of symmetrically substituted and of the subtransition of asymmetrically substituted phosphatidylcholines. The use of the dye for the elucidation of the kinetics of these phase transitions by relaxation spectrometry is discussed.

Useful information about lipid organization and dynamics in both model and biological membranes has been obtained from studies that employ lipid probes. These probes may contain paramagnetic groups for electron paramagnetic resonance studies (Seelig, 1970; Gaffney & McConnell, 1974), nuclei such as deuterium (Seelig, 1977), carbon-13 (Wittebort et al., 1981, 1982), and fluorine (Sturtevant et al., 1979) for NMR[1] investigations, or chromophores for fluorescence measurements (Azzi, 1975; Radda, 1975; Sklar et al., 1977, 1979).

For the investigation of lipid phase transitions, fluorescent probes have been widely used. For instance, the fluorescent *trans*-parinaric acid preferentially partitions into the gel phases (Sklar et al., 1977, 1979). Hence, the liquid crystalline to gel phase transition induces a strong increase of fluorescence intensity of this probe. In this paper, we report the properties of an anthracenophane cryptand that monitors with comparable sensitivity the first gel phase transition of lecithins below the main transition, i.e., the pretransition of symmetrically substituted phosphatidylcholines (Janiak et al., 1976; Chapman et al., 1977) and the subtransition of asymmetrically substituted phosphatidylcholines (Stümpel et al., 1983). The anthracenoyl dye shows a pronounced affinity for the phases L_ϵ and L_β of lecithins. For the synthesis of the cryptand and two other fluorescent dyes, anthracene moieties were covalently linked in 9,10 position to cyclic polyethers. The anthracene group has already been employed for a set of (9-anthroyloxy)$_n$ fatty acids, which allowed one to label the bilayer at defined positions within the bilayer leaflet (Thulborn & Sawyer, 1978; Haigh et al., 1979). These probes have been used to estimate membrane fluidity gradients (Tilley et al., 1979; Vincent et al., 1982).

In this paper we describe the syntheses of the anthracene crown compounds and cryptands (Figures 1 and 2) and their complexation properties and characterize their interaction with sonicated DMPC vesicles by the relative quantum yields, lifetimes, fluorescence anisotropies, binding and fluorescence quenching experiments, and equilibrium cooling curves. Changes of vesicle morphology show up in NMR and electron microscopy experiments. The properties of the anthracenophane cryptand were investigated in detail because the dye turned out to be an excellent reporter group for monitoring the relaxation kinetics of phase transitions between the gel states of lecithins.

Materials and Methods

Synthesis of 1,12,23,34-Tetraoxo-2,11,24,33-tetraaza-5,8,27,30,47,50,55,58-octaoxa[12.8^{2,11}](9,10)anthraceno[12.8^{24,33}](9,10)anthracenophane (III). (*A*) *9,10-Dibromoanthracene* (**1**) was synthesized as described in the supplementary material (see paragraph at end of paper regarding supplementary material).

(*B*) *9,10-Anthracenedicarboxylic Acid* (**6**) *and 9,10-Anthracene Acid Chloride* (**7**). A total of 3.00 g (47.7 mM) of *n*-butyllithium was added under nitrogen to a suspension of 5.00 g (14.9 mM) of 9,10-dibromoanthracene in 30 mL of absolutely dried diethyl ether. The mixture was stirred for 15 min at room temperature. The dark yellow dilithium salt precipitated. The reaction mixture was poured on dry ice. After the addition of water and diethyl ether, the aqueous

† From the Zentrum Biochemie, Abteilung Biophysikalische Chemie, Medizinische Hochschule Hannover, D-3000 Hannover 61, West Germany (U.H., B.T., and G.M.), and the Institut für Organische Chemie und Biochemie der Universität Bonn, D-5300 Bonn 1, West Germany (P.K.T.M. and F.V.). *Received August 18, 1983.* This work was supported by grants from the Deutsche Forschungsgemeinschaft and the Fonds der Chemischen Industrie.

[1] Abbreviations: CD, circular dichroism; DMA, 9,10-dimethylanthracene; DPH, 1,6-diphenylhexa-1,3,5-triene; DMPC, dimyristoylphosphatidylcholine; DPPC, dipalmitoylphosphatidylcholine; 1M-2S-PC, 1-myristoyl-2-stearoylphosphatidylcholine; NMR, nuclear magnetic resonance; PL, phospholipid; 1S-2M-PC, 1-stearoyl-2-myristoylphosphatidylcholine.

0006-2960/84/0423-4059$01.50/0

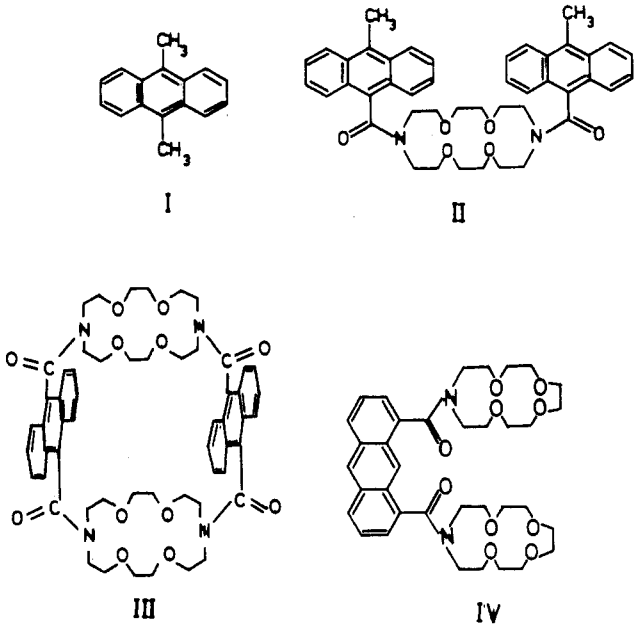

FIGURE 1: Structural formulas of 9,10-dimethylanthracene and its crown ether derivatives.

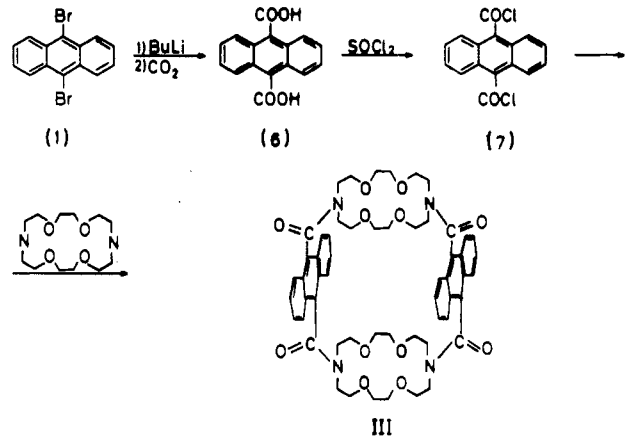

FIGURE 2: Reaction scheme for the synthesis of the anthracenophane cryptand III.

phase was separated and acidified with diluted sulfuric acid, and the resulting yellow product was filtered off. The recrystallization from diluted ethanol yielded 4.00 g (72%) of yellow crystals of **6** (mp 330 °C dec; Mikhailov, 1948). The corresponding acid chloride **7** was obtained by refluxing the dicarboxylic acid **6** with thionyl chloride for 2 h. After removal of excessive $SOCl_2$ by vacuum distillation, intermediate **7** was used without any further purification for the synthesis of the final product (III).

(*C*) *Anthracenophane* (*III*). A total of 0.75 g (2.5 mM) of the acid chloride **7** and 1.31 g (5.0 mM) of "diaza-18-crown-6" (**5**) dissolved separately in 250 mL of absolutely dried benzene were dropped within 7 h to 1 L of vigorously stirred benzene under N_2 atmosphere. After the removal of the precipitated salt by filtration, the filtrate was evaporated to dryness in vacuum. The remaining oil solidified upon the addition of diethyl ether and was filtered off. Several cycles of boiling in diethyl ether and of filtration finally yielded 1.15 g (92%) of a slightly yellow powder of anthracenophane III: mp 185–192 °C; ^1H NMR ($CDCl_3$) δ 7.84 and 7.51 (AA', BB', 16 H, CH phenylene), 4.33–2.56 (m, 48 H, CH_2). Anal. ($C_{56}H_{64}N_4O_{12}$) C, H, N.

The syntheses of the ligands II and IV are described in the supplementary material.

Membrane Studies and Studies on the Structure and Complexation of Ligands. (*A*) *Materials.* The purity of all samples of the complexing dyes was checked by thin-layer chromatography. All salts and solvents were of the highest grade commercially available (p.a. or suprapur, Merck). Contaminations of the saline solutions by transition metal ions (Mn, Co, Ni, Fe) were checked by flameless atomic absorption spectrometry. The upper limit of allowed Mn^{2+} contamination was set to 0.1 and 1 ppm for stock solutions of alkali and alkaline earth metal ions, respectively. DMPC (Fluka) ran as one spot in thin-layer chromatography and was used without further purification. There was no lysolipid or free fatty acid detectable (<1%). The glassware used for the preparation and storage of vesicle dispersions was rinsed extensively with acetone, methanol, EDTA solutions, distilled water, and triple quartz-distilled water.

(*B*) *Spectroscopic and Complexing Properties of the Ligands.* Spectra of the ligands and their complexes with metal ions were monitored by NMR (WH-270, Bruker), absorption (PM QII, DMR 10, Zeiss), fluorescence polarization, and fluorescence spectroscopy (RRS 1000, Schoeffel). Stoichiometry and stability constants were evaluated from spectrofluorometric titrations by a nonlinear curve-fitting procedure as described previously (Tümmler et al., 1979).

(*C*) *Vesicle Preparation.* Small single-lamellar vesicles were prepared by sonication of the lipid following a modification of Huang's procedure (Huang, 1969; Lentz et al., 1976). During preparation and storage, the vesicle dispersions were maintained 20 °C above the temperature of the main phase transition. Some vesicle dispersions were made homogeneous in size (r = 105 ± 20 Å) by a second centrifugation step of the supernatant at 150000*g* for 4 h (Barenholz et al., 1977). Both types of vesicle preparations showed the same interaction with the various fluorophores.

(*D*) *Tests of Homogeneity of the Vesicle Dispersions.* The contamination by large, multilamellar vesicles was routinely checked in 24h intervals by plotting the turbidity $A(\lambda)$ between 300 and 700 nm vs. the reciprocal fourth power of the scattering wavelength (Barrow & Lentz, 1980). Furthermore, each vesicle preparation was characterized by an equilibrium transition curve at a uniform cooling rate of 0.2 °C min^{-1}, monitoring the turbidity at 300 nm. Gel filtration chromatography with Sephadex CL-4B exhibited one internal volume peak corresponding to Huang's peak II, the fraction of unilamellar vesicles (Huang, 1969), which demonstrates that the preparations were not contaminated to significant extent by multilamellar vesicles. Negative-stain electron microscopy analysis revealed a mean vesicle radius of about 110 Å (cf. Figure 5A).

(*E*) *Fluorescence Quench Titrations.* The quenching of the fluorescence of the anthracenoyl dyes I–IV in DMPC dispersions by Cu^{2+}, SCN^-, and uncharged *N,N*-dimethylaniline was determined by titrations at 10 (phase L_β), 17 (P_β), and 40 °C (L_α), varying the quencher concentration between 0 and 10 mM (Thulborn & Sawyer, 1978). The partition coefficient K_p of *N,N*-dimethylaniline between DMPC and aqueous phase was estimated from sets of quenching titrations with the individual dyes, varying the ratio V_L/V_T of DMPC to total volume between 10^{-4} and 2×10^{-3} and the quencher concentration between 0 and 2 mM. The values of K_p and of the rate constant k_q of the association of dye and quencher were determined from plots according to (Sikaris et al., 1981)

$$\frac{I}{I_0 - I}[Q_T] = \frac{1}{k_q \tau}\frac{V_L}{V_T} + \frac{1}{k_q K_p \tau} \qquad (1)$$

Table I: Apparent Stability Constants (M^{-1}) of Metal Ion Complexes of Dyes II–IV ($K_{app} = M^{-1}$)

solvent	dye	const	salt		
			NaSCN	KSCN	$Ca(SCN)_2$
50% CH_3OH/50% $CHCl_3$	II	K_1[a]			$(5 \blacksquare 2) \times 10^4$
50% CH_3OH/50% $CHCl_3$	III	K_1	$\simeq(10^4$	$\simeq 10^4$	$(2 \pm 1) \times 10^4$
50% CH_3OH/50% $CHCl_3$	III	K_2	150 ±50	70 ±20	$\simeq 10^3$
ethyl acetate	II	K_1			$(3 \pm 2) \times 10^4$
ethyl acetate	III	K_1			$(8 \pm 1) \times 10^3$
acetonitrile	III	K_1			$(2 \pm 1) \times 10^5$
acetonitrile	III	K_2	$(1.5 \pm 0.5) \times 10^2$	60 ± 30	$(8 \pm 3) \times 10^2$
acetonitrile	IV	K_1		$(2 \pm 1) \times 10^3$	$(1 \pm 0.5) \times 10^5$
acetonitrile	IV	K_2	40 ± 20	30 ± 20	$(2.3 \pm 0.3) \times 10^2$

[a] K_1, first binding site; K_2, second binding site.

I and I_0 are the fluorescence in the presence and absence of quencher; τ is the fluorescence lifetime.

(F) Lifetime Measurements. Fluorescence lifetimes were determined by measurements of the phase lag and of the relative modulation of the emitted light in an SLM 4800 fluorometer equipped with light modulator LH 480. The operating modulation frequencies were 18 and 30 MHz. The component lifetimes of heterogeneous emitting populations were evaluated according to the resolution theory developed by Weber (1981).

Studies on Membrane Fusion. (A) ^1H NMR Experiments (WH-270, Bruker). The fusion of sonicated small vesicles prepared in 10 mM NaCl/D_2O was observed by following the time-dependent change of choline methyl protons at 50 °C after the addition either of 2 mM $MnSO_4$ in D_2O alone (Bystrov et al., 1971; Hutton et al., 1977) or of 2 mM $MnSO_4$ together with 2 μM anthracenophane III in CD_3CN. The HDO signal was taken as a reference peak.

(B) Electron Microscopy. For negative staining, aliquots of vesicle preparations in 70 mM $CaCl_2$ with and without ligand III were kept at 50 °C or cooled down to 24 or 0 °C (0.2 °C min^{-1}). The samples were placed on carbon-coated grids and mixed with a 10% (v/v) solution of phosphotungstic acid (pH 7) of the same temperature. For freeze–fracture experiments, vesicle solutions in 70 mM $CaCl_2$ were slowly mixed with increasing amounts of glycerol up to a final 30% solution (v/v) and then slowly cooled down to 0 °C. The cryofixation was performed on gold plates in Freon 22 at −150 °C. A Balzer 360 M instrument was used for fracturing, etching, and platinum–carbon shadowing. The replicas (thickness 2.5 nm) were floated on water and washed several times with water and dimethylformamide. Replicas and grids were examined in a Siemens 101 electron microscope at an accelerating voltage of 80 kV.

(C) Equilibrium Cooling Curves. A 2-μL aliquot of a 1 mM stock solution of anthracenoyl dye in tetrahydrofuran was added under rapid vortexing to 5 mL of the vesicle dispersion diluted to a concentration of 0.3–1.6 mM phosphatidylcholine. The solution was incubated for 2–3 h at 20 °C above T_m. The cooling curve was recorded with a rate of 0.05–0.2 °C min^{-1}, monitoring the fluorescence polarization or the fluorescence intensity of the anthracenoyl dye (λ_{Ex} = 373 nm; λ_{Em} = 425 nm) against a fluorophore standard and a blank of the vesicle dispersion.

Results and Discussion

Syntheses of the Anthracenoyl Crown Compounds and Cryptands. The three synthesized ligands II–IV differ with respect to the number of crown ether units and the stereochemical arrangement of crown ether and fluorophore. The similarity of the structural design is reflected in similar strategies for the synthesis of the molecules. Starting from anthracene or 1,8-dichloroanthraquinone, the anthracenecarboxylic acids were synthesized via halogen or pseudohalogen intermediates. The reaction of the corresponding acid chlorides with the diaza crown compound yielded the final products. In contrast to the common route of coronand and cryptand syntheses, the acid amides were not reduced to the corresponding amines, thereby avoiding the generation of positive charges within the molecules that would impair the binding or uptake of the ligands by lipophilic environments. On the other hand, the maintenance of the amide groups considerably restricts the flexibility of the ligands due to the hindered rotation around the C–N amide bonds; in the case of ligand IV, the free activation enthalpy of rotation around the C–N amide was determined from the temperature dependence of its ^{13}C NMR spectrum to be $\Delta G_c^* = 74$ kJ mol^{-1} at 361 K.

Complexation of Alkali and Alkaline Earth Metal Ions by the Ligands. The complexation of Na^+, K^+, and Ca^{2+} by the ligands II–IV was measured in methanol, acetonitrile, ethyl acetate, and a methanol/chloroform mixture (1/1 v/v), monitoring the quench of the anthracene fluorescence. The uptake of the first alkali or alkaline earth metal ion was accompanied by a 3–6% fluorescence quench depending on solvent, ligand, and salt. The small quench indicates that in the 1:1 complex only weak interactions between cation and fluorophore occur. On the other hand, when the second binding site of ligands III and IV was occupied by a cation, the fluorescence decreased considerably by another 30–70% of the initial signal, which demonstrates that in the conformation of the 1:2 complex the bound cations interact more strongly with the anthracenes.

The stability constants K_{app} of the complexes were evaluated from spectrofluorometric titrations (Table I). For the 1:1 complexes, the small quench restricted the accuracy of the experimental binding curves. Therefore, only the order of magnitude of K_{app} could be reliably determined. The values of the 1:1 Na^+ and K^+ complexes are in the range of 10^4–10^5 M^{-1}. The stability constants of Na^+, K^+, and Ca^{2+} for the second binding site of ligands III and IV are 2–3 orders of magnitude smaller than for the first binding site. Calcium ions are bound 5–20-fold stronger than sodium and potassium ions.

Studies on Model Membranes. (A) Uptake Kinetics. The uptake of the ligands I–IV by DMPC vesicles at 15, 35, 45, and 60 °C was measured by continuous monitoring of the fluorescence after the addition of 2 μL of the 1 mM stock solution of the ligand in tetrahydrofuran to 2 mL of the vesicle dispersion. Depending on the temperature and the ligand chosen, 90–99% of the final fluorescence signal was reached within less than 1 s. In case of the compounds I–III, the initial binding step was followed by a slower process of a half-time between 1 and 10^2 s. The variation of salt (NaCl, KCl, $MgCl_2$, $CaCl_2$) and ionic strength (2, 10, 50, 200, and 500 mM) had

Table II: Relative Quantum Yields (ϕ) and Fluorescence Lifetimes (τ) of the Anthracenoyl Dyes

dye	τ (ns) in THF (δ = 25 °C)	τ (ns) in DMPC vesicle dispersions δ = 10 °C	τ (ns) in DMPC vesicle dispersions δ = 17 °C	τ (ns) in DMPC vesicle dispersions δ = 40 °C	ϕ(dye)/ϕ(DMA) in DMPC vesicle dispersions (δ = 25 °C)[a]
I	7.1 ± 1.4	15.3 ± 0.4	15.1 ± 0.4	14.5 ± 0.5	1.0
II	7.4 ± 0.5	12.2 ± 0.5	11.5 ± 0.4	10.1 ± 0.3	2.0
III	6.8 ± 0.3	11.8 ± 0.5	11.6 ± 0.5	11.3 ± 0.7	0.12[b]
		2.9 ± 0.5	2.8 ± 0.5	2.8 ± 0.7	0.4[c]
IV	7.1 ± 0.2	3 ± 1	2.6 ± 0.6	2.4 ± 0.5	0.01

[a] The data are given for a dye concentration of 0.5 μM and a DMPC concentration of 1 mM. Comparative value: ϕ(DMA in H_2O)/ϕ(DMA in vesicle dispersion of 1 mM DMPC) = 0.01. [b] δ = 40 °C. [c] δ = 0 °C.

Table III: Quenching of the Anthracenoyl Dyes by *N,N*-Dimethylaniline in DMPC Vesicles[a]

dye	$10^{-8}k_q$ (M^{-1} s^{-1}) δ = 10 °C	$10^{-8}k_q$ (M^{-1} s^{-1}) δ = 17 °C	$10^{-8}k_q$ (M^{-1} s^{-1}) δ = 40 °C	K_p δ = 10 °C	K_p δ = 17 °C	K_p δ = 40 °C
I	0.6 ± 0.1		1.4 ± 0.2	270 ± 50		250 ± 50
II	0.3 ± 0.1		0.4 ± 0.1	180 ± 40		150 ± 50
III	0.8 ± 0.1	0.9 ± 0.2	1.4 ± 0.2	250 ± 50	220 ± 50	<50

[a] The bimolecular rate constant k_q and the partition coefficient K_p were evaluated from plots according to eq 1. The ratios $10^3V_L/V_T$ for the quenching titrations were chosen to be 0.1, 0.25, 0.5, 1.0, 1.5, and 2.0.

no detectable influence on the uptake kinetics.

(*B*) *Binding of the Anthracenophane III by Aqueous DMPC Dispersions.* The association constant K_{app} for the binding of one anthracenophane molecule per vesicle was determined from sets of spectrofluorometric titrations at 0 (phase L_β), 19 (phase P_β), and 40 °C (phase L_α), varying the dye concentration between 0.1 and 20 μM and the lecithin concentration between 5 μM and 2 mM DMPC. As an example, Figure 3a displays the binding curves with 0.39 mM DMPC. The binding constant K_{app} expressed per mole of DMPC was determined to be $K_{app} = (5.4 \pm 1.3) \times 10^2$ M^{-1} at 0 °C, $(1.3 \pm 0.3) \times 10^2$ M^{-1} at 19 °C, and about 50 ± 20 M^{-1} at 40 °C. The ratio of the relative fluorescence intensities at 0 and 40 °C as a function of the dye concentration is shown for various DMPC concentrations in Figure 3b. The figure reveals that the optimum concentrations for the resolution of the temperature-dependent change of fluorescence intensity are 0.1–1 μM fluorophore and above 0.1 mM DMPC.

(*C*) *Lifetimes and Relative Quantum Yields.* The data for the various fluorophores in 1 mM DMPC dispersions are given in Table II. The lifetime measurements by phase lag and by the modulation of the amplitude yielded the same values for the dyes I, II, and IV, which is sufficient proof that the emitting populations are homogeneous and are located to more than 95% either in the lipid phase (I and II) or in the aqueous phase (IV). On the other hand, two lifetimes of 3 and 12 ns were resolved for 1 μM anthracenophane III, which correspond to the values in the aqueous and lipid phase, respectively. At 4 °C the fast-decaying lifetime component contributed to about 10% to the total fluorescence intensity. Since the quantum yield of anthracene dyes is 100-fold higher in lecithin than in water, the amount of the anthracenophane dissolved in the aqueous phase is estimated to be 90%, which agrees with the value calculated from the binding constant of 540 M^{-1}.

(*D*) *Fluorescence Quench Titrations.* The distribution of the anthracenoyl dyes between aqueous and lipid phases and their relative location across the bilayer were approximately determined by fluorescence quench titrations with Cu^{2+}, SCN^-, and the neutral form of *N,N*-dimethylaniline. Cu^{2+} and SCN^- ions distribute in the aqueous phase and in the polar part of the lecithin bilayer, whereas *N,N*-dimethylaniline partitions into the whole DMPC bilayer (Sikaris et al., 1981). Copper ions and *N,N*-dimethylaniline have already been employed for Stern–Volmer titrations of (9-anthroyloxy)$_n$ fatty acids (n = 2, 6, 9, 12, or 16) in DMPC bilayers (Thulborn & Sawyer, 1978). *N,N*-Dimethylaniline exhibits an anisotropic distribution across the bilayer. The maximum of the partition coefficient K_p between lipid and aqueous phase is in the bilayer center, a second relative maximum is near the glycerol backbone, and in going from C-2 to C-12, K_p monotonously decreases. Hence, if quenching titrations with mobile anthracenoyl dyes and *N,N*-dimethylaniline are performed and the calculated partition coefficient K_p is compared with the values obtained from the calibration with the (anthroyloxy)$_n$ fatty acids, the average location of the mobile fluorophore in question can be determined.

Table IV: Fractional Maximum Fluorescence of the Anthracenoyl Dyes Accessible to Quenching by NaSCN and *N,N*-Dimethylaniline in Aqueous DMPC Vesicle Dispersions[a]

dye	NaSCN 10 °C	NaSCN 40 °C	*N,N*-dimethylaniline 10 °C	*N,N*-dimethylaniline 40 °C
I	<0.01	<0.01	>0.9	0.77 ± 0.07
II	0.26 ± 0.02	0.55 ± 0.08	>0.9	>0.9
III	0.73 ± 0.05	0.72 ± 0.05	0.76 ± 0.05	0.73 ± 0.06
IV	<0.01	<0.01	<0.01	<0.01

[a] The vesicle dispersions contained 0.5 mM DMPC and 2 μM fluorophore.

Figure 4 displays the quenching behavior of the anthracenoyl dyes I–III with NaSCN and *N,N*-dimethylaniline over the concentration range of 0–10 mM. The copper ions behaved qualitatively similar as thiocyanate; however, the quenching efficiency was as low as it was measured for the (anthroyloxy)$_n$ fatty acids. For the determination of K_p values of *N,N*-dimethylaniline, titrations were performed in the approximately linear range of the Stern–Volmer plot between 0 and 2 mM quencher. By varying the lipid concentration, we were able to plot the data according to eq 1, and k_q was calculated from the slopes. For the determination of K_p, the data had to be corrected for the contribution from static quenching. Since the equilibrium complex between the quencher and the ground state of the fluorophore disappears at infinitely small concentrations, the ordinate intercepts of plots according to eq 1 were replotted vs. quencher concentration and extrapolated to 0. The extrapolated value gives a good estimate of the partition coefficient (Sikaris et al., 1981). The values of K_p and k_q are summarized in Table III. The percentage of the anthracenoyl dyes accessible to the quench by NaSCN and *N,N*-dimethylaniline was determined from plots $I_0/(I_0 - I)$ vs. $[Q]^{-1}$ (Lehrer, 1971). As shown in Table IV, the fluorescence

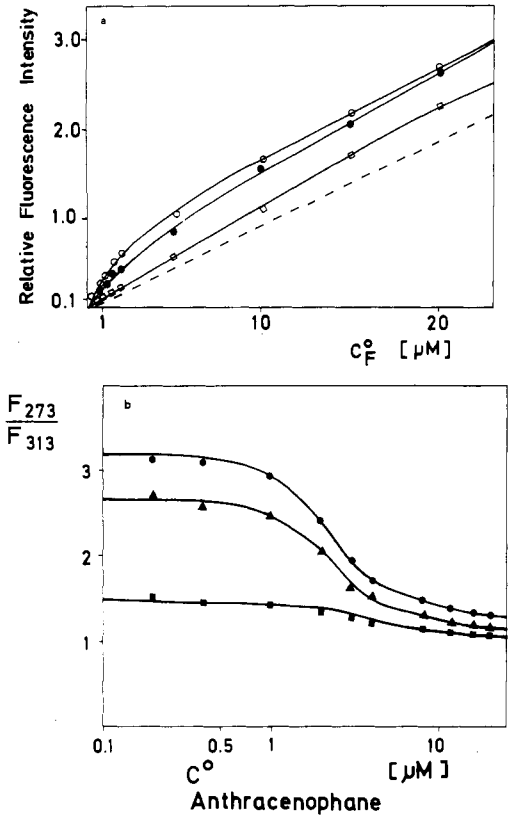

FIGURE 3: (a) Spectrofluorometric titrations of the binding of anthracenophane III at 273 (phase L_β, open circles), 292 (phase P_β, closed circles), and 313 K (phase L_β, open squares) to an aqueous dispersion of 0.39 mM DMPC. The dashed line indicates the relative fluorescence intensity of the anthracenophane in water. (b) Ratio of the relative fluorescence intensity of the anthracenophane III at 273 and 313 K in aqueous DMPC dispersions as a function of the concentration of the anthracenoyl dye. The DMPC concentrations are 0.3 (circles), 0.09 (triangles), and 0.01 mM (squares).

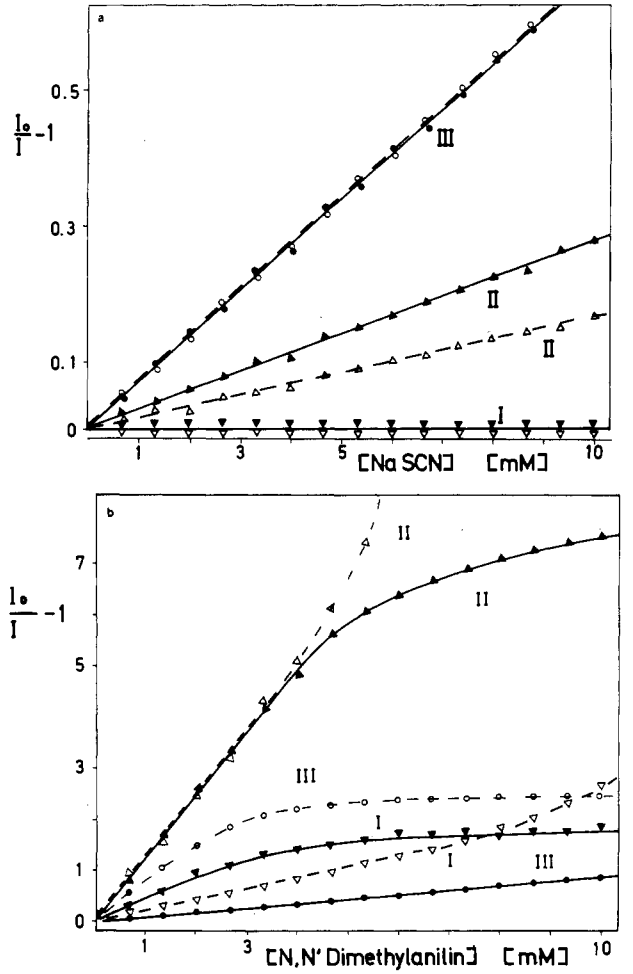

FIGURE 4: Stern–Volmer plots of the quenching of DMA (I) and the crown ether derivatives II and III in 1.6 mM DMPC dispersions (50 mM NaCl) at pH 6.8 by NaSCN (a) and *N,N*-dimethylaniline (b) at 10 (broken line) and at 40 °C (solid line). The plots with NaSCN were corrected for the specific uptake of sodium ions into the binding sites of the crown compounds by control titrations with NaCl in the concentration range of 50–60 mM.

of the individual dyes could not be completely quenched. Several facts account for this phenomenon, which has already been reported for the $(anthroyloxy)_n$ fatty acids (Thulborn & Sawyer, 1978): the binding sites of the phospholipid for the quencher become saturated, the concentration profiles across the bilayer of quencher and fluorophore do not coincide, and in the case of the dyes III and IV, the majority of the fluorophores is still in the aqueous phase. These effects, however, are of no relevance for the validity of the K_p determinations of *N,N*-dimethylaniline because the titrations were performed with low concentrations of quencher where only static quenching caused the nonlinearity of the Stern–Volmer plot. Static quenching was eliminated by the extrapolation to zero quencher concentration (vide supra).

In the case of DMA (I), the fluorescence is not quenched by thiocyanate, and for *N,N*-dimethylaniline, K_p has its maximum of about 250 at 10 and 40 °C. Therefore, it can be concluded that in the solid and fluid phases DMA is concentrated at the center of the bilayer. On the other hand, the fluorescence of dye II can be quenched by SCN^-, and K_p has a value between 150 and 200; consequently, the anthracene residues of II are assumed to be located in the more polar part of the acyl chain near the glycerol backbone. A different situation holds for the anthracenophane III. Above and below T_m the fluorophores are accessible to the same extent to thiocyanate; hence, the anthracenophane molecules are located in the polar part of the phospholipid molecule, irrespectively of whether the membrane is in the gel or in the fluid state. As indicated by the shift of K_p of dimethylaniline, however, the average position of the dye changes discontinuously during the main transition. At 40 °C in phase L_α, K_p was determined to be smaller than 50. In the P_β phase at 17 °C and in the L_β phase at 10 °C, however, K_p values of 200–250 were found, which correspond to a position of the fluorophore at the polar end of the acyl chain. Hence, we conclude that during the transition from the gel to the liquid crystalline state the average location of membrane-bound anthracenophane III shifts from the glycerol backbone to the choline head groups. If we chose DMPC concentrations of up to 10 mM, the most hydrophilic ligand IV was not incorporated into the hydrocarbon phase. Its fluorescence in 1 mM DMPC dispersions was comparable to that in the bulk aqueous solution, and hence, this very low quantum yield due to the solvent quench could not be further quenched by $CuSO_4$, NaSCN, and *N,N*-dimethylaniline.

(*E*) *Fluorescence Anisotropy of the Anthracenophane III.* The anisotropy *r* of the anthracenophane III was measured in propylene glycol at −14 °C at the maxima of the absorption spectrum. At this temperature, the viscosity of the solvent is in the same range usually ascribed to membranes (Shinitzky, & Barenholz, 1978), although the limits of validity of this parameter for the characterization of membranes are already known (Kinosita et al., 1977; Hare et al., 1979). The values of *r* at 338, 356, 374, and 395 nm were determined to be 0.060, 0.073, 0.091, and 0.105. At this temperature, the anisotropies of the reference compounds DPH and of $(anthroyloxy)_n$ fatty

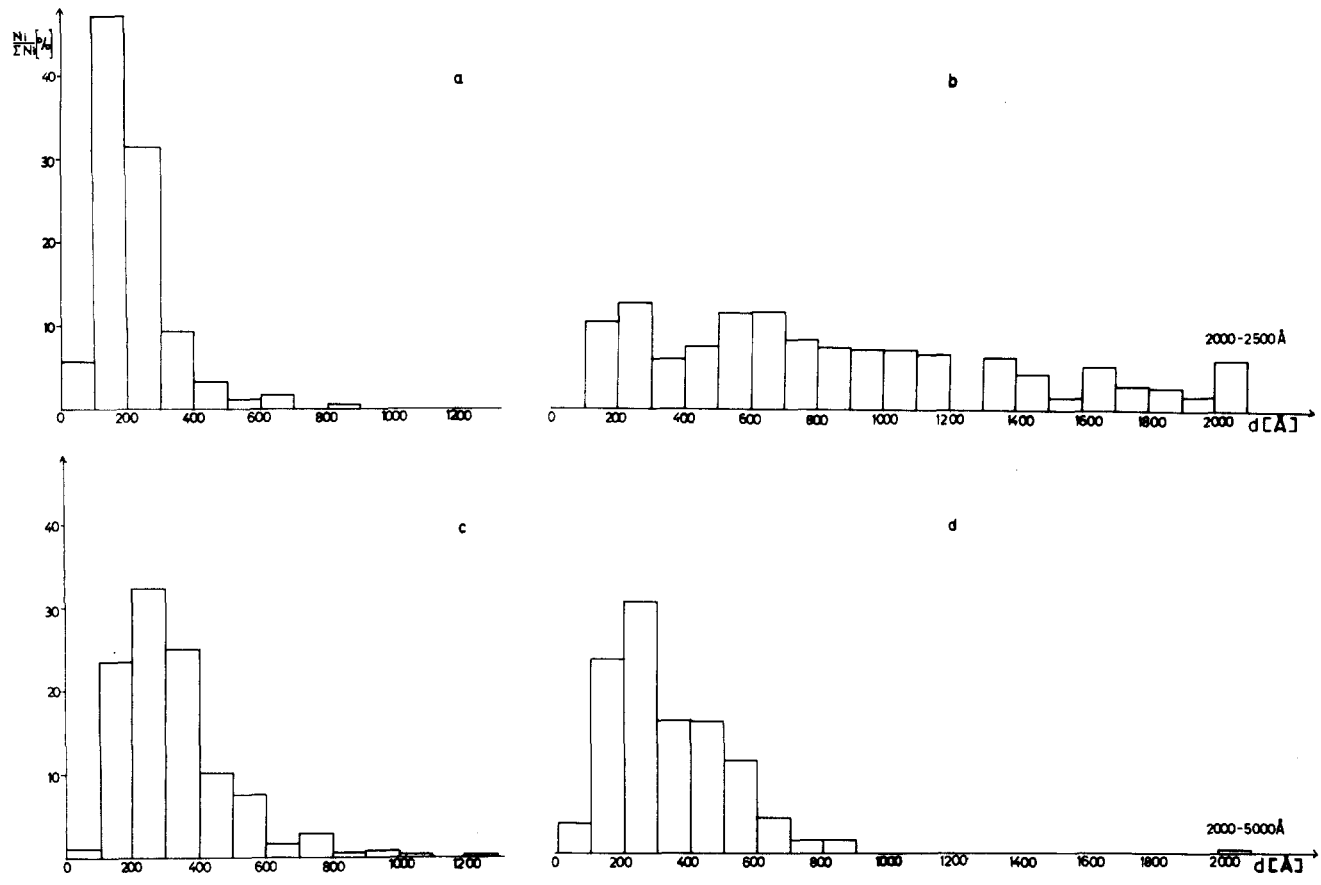

FIGURE 5: Histograms of DMPC vesicle diameters measured from electron micrographs of sonicated DMPC vesicle dispersions (2.8 mM DMPC) in 70 mM $CaCl_2$ fixed and negatively stained with phosphotungstic acid at (a and b) 40 and (c and d) 0 °C in the presence (b and d) and absence (a and c) of 1 μM anthracenophane probe III. A total of (a) 662, (b) 572, (c) 647, and (d) 361 vesicles was measured.

acids amount to about 75% of the corresponding fundamental anisotropy r_0 (personal data; Prendergast, 1981; Vincent et al., 1982). Hence, the maximum r_0 value of the anthracenophane is estimated to be not larger than 0.14, which is far less than the limiting anisotropy of 0.4. We conclude that there exists no parallel orientation of the absorption and emission oscillators for the long-wavelength absorption band as it is observed for DPH and anthracene monomers (Weber, 1971; Vincent et al., 1982; Yguerabide & Foster, 1981), presumedly because the intramolecular electronic interaction between the two anthracene residues in the phane molecule may lead to a different angle of the transition dipoles as compared to the isolated monomers (Merzbacher, 1970). Since even for the highest excitation wavelenghts the anisotropies of the anthracenophane are small, the resolution of the equilibrium cooling curves for the detection of phospholipid phase transition is poor when the temperature-dependent change of the anisotropy of dye III is chosen as the observed parameter.

(F) Fusion of Single-Lamellar DMPC Vesicles Induced by the Anthracenophane. Figure 5 shows the histograms of the size distribution of vesicle preparations at 0 and 50 °C in the presence or absence of ligand III (c = 1 μM) as revealed by electron microscope photographs. If we assume 3×10^3 lipid molecules per sonicated vesicle (Watts, 1978), the ratio of ligands per vesicle was set to about 2:1 to 1:1. Without ligand, the dispersions consisted at 50 °C of small single-lamellar vesicles of a mean radius of 11 nm and of a small fraction of medium-sized vesicles of a maximum diameter of 70 nm (Figure 5a). In presence of the anthracenophane III, a very broad continuous size distribution of single-lamellar vesicles 20–250 nm in diameter was observed (Figure 5b). This finding demonstrated that the anthracenophane III induces the fusion of the small unilamellar vesicles to larger vesicles. Above T_m no preference for a defined vesicle size was observed. On cooling from 50 to 0 °C, the absolute number of small and medium-sized vesicles per unit area decreased. Already at T_m (24 °C) the DMPC dispersions consisted of two separate populations of small vesicles and larger irregularly shaped structures. Only a small number of some isolated macrovesicles was still detectable. At 0 °C, the macrovesicles 80–200 nm in size had vanished completely. Instead, more than 50% of the total lipid mass was located in large lipid structures approximately 0.2–1 μm in size. These structures were identified by freeze–fracture electron microscopy as multilamellar lipid–water structures highly irregular in shape and contour. In the presence of the anthracenophane, the single-lamellar vesicles, especially the largest macrovesicles, became unstable in the gel phase and fused to coacervates. In the control preparations without anthracenophane, no lipid coacervates at 0 °C were observed.

The fusion of the sonicated DMPC vesicles was also detected in ^1H NMR spectra by observing the line broadening of the methyl resonances of the inner choline head groups by manganese ions (Bystrov et al., 1971; Hutton et al., 1977). Since DMPC microvesicles are permeable to Mn^{2+} (Dufour et al., 1981), control experiments in the absence of ligand III were performed yielding a half-time of line broadening of $t_{0.5} = 7 \times 10^2$ s at 40 °C (Figure 6). In the presence of the anthracenophane, the half-time shortened to 3×10^2 s, indicating that due to the fusion of the vesicles the permeation of manganese ions into the interior of the vesicles was accelerated (Figure 6). No fusion was observed when the single-lamellar DMPC vesicle dispersions were incubated with the other anthracene derivatives I, II, and IV.

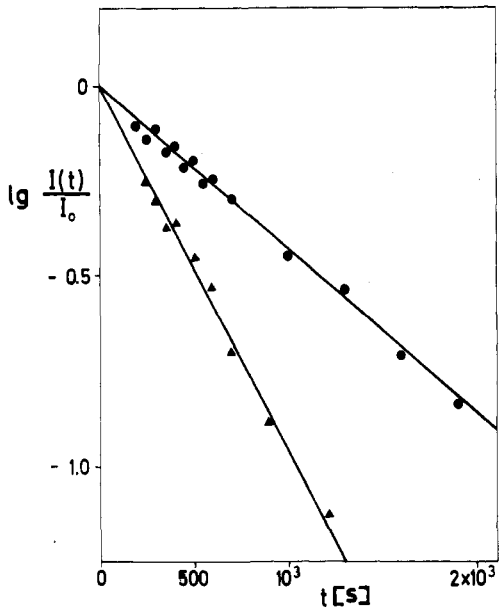

FIGURE 6: Penetration of $MnSO_4$ in sonicated DMPC vesicles at 50 °C in the presence (triangles) and absence (circles) of the anthracenophane III. Vesicles (9.2 mM DMPC) were prepared in 10 mM $NaCl/D_2O$. At time zero, either solely $MnSO_4$ or $MnSO_4$ plus dye III were added to the sample to 10 mM and 1 μM final concentration of salt and probe. Each point represents an average value of the time required for one 270-MHz ^1H NMR spectrum (10 scans, τ = 4 s, AT = 1 s). For each spectrum, the intensity of the peak of the [^1H]methyl signals of the inner choline head groups was integrated.

Phase Transitions of Aqueous Dispersions of DMPC Monitored by the Anthracenoyl Dyes. In both turbidity and DMA fluorescence the vesicle preparations displayed one broad symmetric transition curve in accordance with literature data (Lentz et al., 1976; Tsong & Kanehisa, 1977; Dufour et al., 1981). The calculation of the cooperative unit $\langle v \rangle$ defined as the ratio of the van't Hoff enthalpy $\Delta H_{vh} = 4RT^2/\Delta T_{0.5}$ to the calorimetrically determined enthalpy ΔH_{cal} (Mabrey & Sturtevant, 1976, 1979) gave values of 11–13, which are characteristic for small unilamellar vesicles (Dufour et al., 1981). The sonicated vesicle dispersions were remarkably stable under our experimental conditions. Repetitive cycles of cooling and heating yielded the same profiles of the transition curve for at least the first two cycles.

A fluorescence cooling curve of DMPC vesicles with the anthracenoyl dye II is displayed in Figure 7. In the liquid crystalline state the fluorescence increased with decreasing temperature, and in the gel state it remained constant. Cooling curves of DMPC vesicles in saline solutions of NaCl or KCl (10, 50, and 200 mM), $MgCl_2$ (50 mM), or $CaCl_2$ (2, 10, 50, and 200 mM) yielded the same temperature profile of the fluorescence of II, which demonstrates that neither the metal ion complexed by the crown ether nor the metal ions bound by the choline head groups affected the polarity and mobility of the microenvironment of the ligand.

A fluorescence cooling curve of DMPC containing the anthracenophane III is also shown in Figure 7. In the liquid crystalline phase 1 μM dye fluoresced in a 1 mM DMPC dispersion only 10 times stronger than in an aqueous saline solution. Below T_m, however, the fluorescence gradually increased by a factor of 3.5 over a temperature range of 20 K. The maximum fluorescence increase occurred at the calorimetrically determined temperature T_p of the pretransition (Chapman et al., 1977). This characteristic difference of the fluorescence signal of the anthracenophane below and above T_m confirms the result of the binding titrations that compound III preferentially partitions into the solidlike conformations

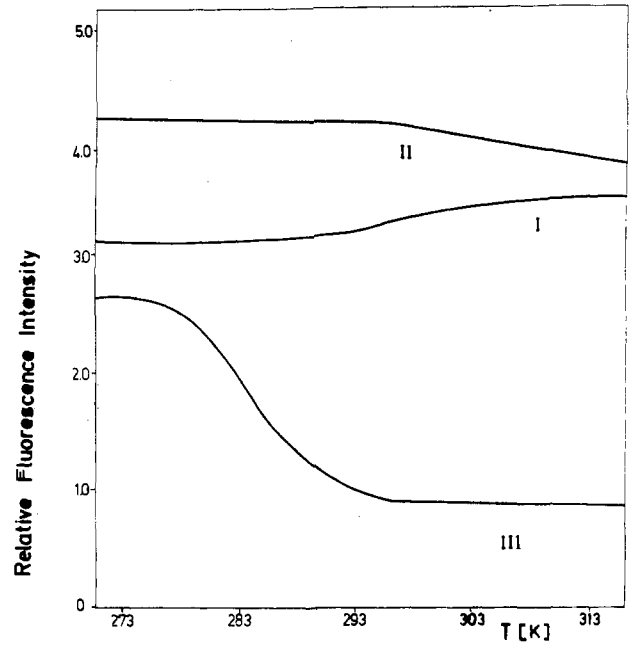

FIGURE 7: Fluorescence intensities of DMA (I) and of the anthracenoyl dyes II and III in 1.6 mM DMPC dispersions (50 mM $CaCl_2$) as a function of temperature (cooling curves).

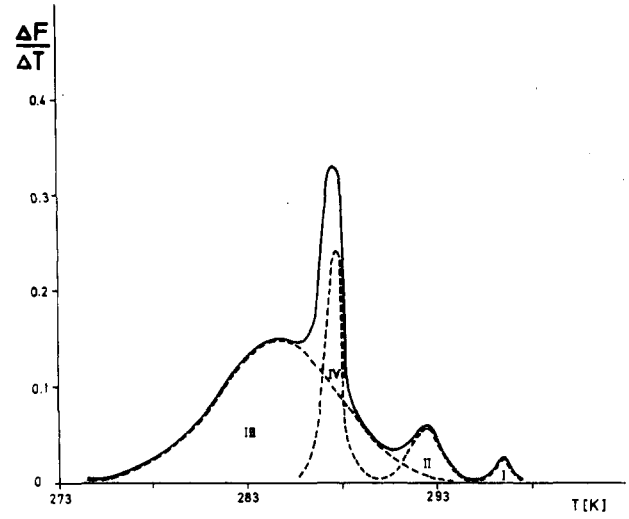

FIGURE 8: Differential change of the fluorescence of the anthracenophane III $\Delta F/\Delta T$ in a DMPC dispersion (1.6 mM PL, 50 mM NaCl) as a function of temperature. The assignment of the transitions I–IV is given in the text.

of the phospholipid. The quench titrations with *N,N*-dimethylaniline revealed that the average location of bound anthracenophane in the bilayer does not change in the gel phases P_β and L_β; accordingly, the quantum yield of bound dyes remains constant in these phases. Therefore, the observed increase of fluorescence over a range of 20 K below T_m is a consequence of the continuous increase of the binding constant of DMPC to the dye by all together 1 order of magnitude (vide supra).

The pronounced fluorescence increase in the gel states allowed the evaluation of differential plots of dF/dT vs. T. Four symmetric transitions could be resolved in all saline solutions containing either NaCl, KCl, or less than 50 mM $MgCl_2$ or $CaCl_2$. In accordance with literature data, the four peaks were assigned as follows (Figure 8). Peak I with a T_m of 24.4 ± 0.3 °C represents the gel to liquid crystalline phase transition as observed in unilamellar macrovesicles, liposomes, and phospholipid–water mixtures (Lentz et al., 1976; Dufour et

al., 1981; Chapman et al., 1977). Transition II (T_m = 19.6 ± 0.4 °C) corresponds to the phase transition of small single-lamellar vesicles. The broad peak III conforms in T_m (12.3 °C) and half-width (v = 80 ± 30) to the pretransition as detected for unilamellar macrovesicles and liposomes by light scattering or fluorescent probes (Lentz et al., 1976; Dufour et al., 1981). The sharp peak IV (T_m = 14.4 °C) with its high cooperative unit of $\langle v \rangle$ = 900 ± 200 matches in position and shape the pretransition of hydrated phospholipid mixtures and multilamellar structures as found in the calorimeter (Dufour et al., 1981; Chapman et al., 1977). Depending on the salt used, the midpoints T_{m3} and T_{m4} of the pretransition shifted up to 3 °C in agreement with calorimetric data.

The transitions shown in the differential cooling curves reflect the fusogenic action of dye III on sonicated DMPC vesicles. However, after the fusion has taken place during the incubation and the first cooling scan, the ligand behaves as a reversible, nonperturbing probe. When repetitive cooling and heating cycles were performed, the fluorescence temperature profile remained unchanged and yielded reproducible values of T_m and of $\Delta T_{0.5}$ that were identical with those detected by nonperturbing techniques as light scattering and calorimetry. This finding leads to the practically important conclusion that due to its large change of the fluorescence in the gel phase of the membrane, the anthracenophane cryptand III can be used as a very sensitive reporter group of the pretransition in lecithin membranes.

Conclusions

As shown above by the cooling curves and the binding and the fluorescence quench titrations, above T_m the anthracenophane cryptand binds with low affinity to DMPC, and the bound dyes are located in the head group region of the lecithin. Below T_m the ligand is taken up into a more apolar environment, and the affinity constant steadily increases with decreasing temperature by all together 1 order of magnitude over a range of 20 K. The maximum relative increase of affinity occurs at the temperature of the pretransition. The fluorescence temperature profile of the cryptand runs in parallel to the relative amount of solidlike lecithin conformations in the phases L_β and P_β as determined by ^{13}C NMR experiments (Wittebort et al., 1982); i.e., the larger the proportion of solidlike conformations, the more anthracenophane molecules partition into the phospholipid.

In addition, electron microscopic and NMR experiments demonstrate the fusogenic action of the anthracenophane on sonicated DMPC vesicles. This property is independent of the preference of the cryptand for the gel states of the membrane. As shown in the accompanying paper (Tümmler et al., 1984), the subtransition of mixed-chain lecithins is detected by the anthracenoyl dye with similar high resolution and sensitivity as the pretransition, and in this case, no fusion of sonicated vesicles takes place. Moreover, control measurements with DPPC dispersions yielded essentially the same results as those described in this paper for DMPC (data not shown). Therefore, we conclude that the anthracenophane cryptand can be used as a sensitive probe for the solid phase transitions of phosphatidylcholines.

Despite extensive X-ray (Tardieu et al., 1973; Janiak et al., 1976, 1979; Stümpel et al., 1983), ^{13}C NMR (Wittebort et al., 1982), ESR (Marsh, 1980; Meier et al., 1982), and Raman and IR studies (Gaber et al., 1978; Cameron et al., 1980, 1981), the molecular description of the pre- and subtransitions is still far from complete. Especially, detailed kinetic studies of these phase transitions are still missing. The kinetics of the main phase transition in dispersions of DMPC and DPPC have been studied by relaxation spectrometry (Träuble, 1971; Tsong, 1974; Tsong & Kanehisa, 1977; Gruenewald et al., 1980; Inoue et al., 1981; Gruenewald, 1982). Up to now the relatively small changes of the signals prevented a thorough kinetic analysis of pre- and subtransition. Taking the highly sensitive anthracenophane III as a mobile reporter group, we have overcome this problem. With monitoring of the fluorescence of the anthracenoyl dye, temperature jumps of 0.07 K are large enough to obtain sufficiently resolved relaxation curves. The main disadvantage of the temperature-jump technique, namely, the possibility of partially disrupting the bilayer membrane as a consequence of the electric discharge, can be completely avoided due to the small fields applied of at most 2 kV/cm, which are far below the minimum critical value of 10 kV/cm (Teissie & Tsong, 1981; Ruf & Grell, 1981). Kinetic investigations on the subtransition in aqueous dispersions of 1M-2S-PC and of 1S-2M-PC monitored by the mobile dye III are presented in the accompanying paper.

Acknowledgments

We thank M. Grube and D. Langowski for their collaboration in the binding and membrane experiments. In addition, we are indebted to Prof. L. Luciano for her aid in the electron microscopy investigations and to M. Fiedler for his support in the NMR experiments.

Supplementary Material Available

Reaction schemes and procedures for syntheses of anthracenoyl dyes II and IV (6 pages). Ordering information is given on any current masthead page.

Registry No. **1**, 523-27-3; **2**, 23674-17-1; **3**, 22023-39-8; **4**, 90866-49-2; **5**, 23978-55-4; **6**, 73016-08-7; **7**, 90764-27-5; **9**, 90866-50-5; **10**, 38366-38-0; **11**, 38378-77-7; **12**, 90885-92-0; I, 781-43-1; II, 90790-66-2; III, 90763-91-0; IV, 90764-28-6; DMPC, 13699-48-4; Na, 7440-23-5; K, 7440-09-7; Ca, 7440-70-2; anthracene, 120-12-7.

References

Azzi, A. (1975) *Q. Rev. Biophys. 8*, 237–316.
Barenholz, Y., Gibbes, D., Litman, B. J., Goll, J., Thompson, T. E., & Carlson, F. D. (1977) *Biochemistry 16*, 2806–2810.
Barrow, D. A., & Lentz, B. R. (1980) *Biochim. Biophys. Acta 597*, 92–99.
Bystrov, V. F., Dubrovina, N. J., Barsukov, L. J., & Bengelson, L. D. (1971) *Chem. Phys. Lipids 6*, 343–350.
Cameron, D. G., Casal, H. L., & Mantsch, H. H. (1980) *Biochemistry 19*, 3665–3672.
Cameron, D. G., Casal, H. L., Mantsch, H. H., Boulanger, Y., & Smith, I. C. P. (1981) *Biophys. J. 35*, 1–16.
Chapman, D., Peel, W. E., Kingston, B., & Lilley, T. H. (1977) *Biochim. Biophys. Acta 464*, 260–275.
Dufour, J. P., Nunnally, R., Buhle, L., & Tsong, T. Y. (1981) *Biochemistry 20*, 5576–5586.
Gaber, B. P., Yager, P., & Peticolas, W. L. (1978) *Biophys. J. 21*, 161–176.
Gaffney, B. J., & McConnell, H. M. (1974) *J. Magn. Reson. 16*, 1–28.
Grünewald, B. (1982) *Biochim. Biophys. Acta 687*, 71–78.
Grünewald, B., Blume, A., & Watanabe, F. (1980) *Biochim. Biophys. Acta 597*, 41–52.
Haigh, E. A., Thulborn, K. R., & Sawyer, W. H. (1979) *Biochemistry 18*, 3525–3532.
Hare, F., Amiel, J., & Lussan, C. (1979) *Biochim. Biophys. Acta 555*, 388–408.
Huang, C. (1969) *Biochemistry 8*, 344–352.
Hutton, W. C., Yeagle, P. L., & Martin, R. B. (1977) *Chem. Phys. Lipids 19*, 255–265.

Inoue, S., Nishimura, M., Yasunaga, T., Takemoto, H., & Toyoshima, Y. (1981) *J. Phys. Chem. 85*, 1401–1405.
Janiak, M. J., Small, D. M., & Shipley, G. G. (1976) *Biochemistry 15*, 4575–4586.
Janiak, M. J., Small, D. M., & Shipley, G. G. (1979) *J. Biol. Chem. 254*, 6068–6078.
Kinosita, K., Kawato, S., & Ikegami, A. (1977) *Biophys. J. 20*, 289–305.
Lehrer, S. S. (1971) *Biochemistry 10*, 3254–3263.
Lentz, B. R., Barenholz, Y., & Thompson, T. E. (1976) *Biochemistry 15*, 4521–4528.
Mabrey, S., & Sturtevant, J. M. (1976) *Proc. Natl. Acad. Sci. U.S.A. 73*, 3862–3866.
Mabrey, S., & Sturtevant, J. M. (1979) *Methods Membr. Biol. 9*, 237–274.
Marsh, D. (1980) *Biochemistry 19*, 1632–1637.
Meier, P., Blume, A., Ohmes, E., Neugebauer, F. A., & Kothe, G. (1982) *Biochemistry 21*, 526–534.
Merzbacher, E. (1970) *Quantum Mechanics*, 2nd ed., Wiley, New York.
Mikhailov, B. M. (1948) *Izv. Akad. Nauk SSSR, Ser. Khim.*, 420–426.
Mikhailov, B. M., & Bronovitskaya, V. P. (1952) *Zh. Obshch. Khim. 22*, 157–162.
Prendergast, F. G., Haugland, R. P., & Callahan, P. J. (1981) *Biochemistry 20*, 7333–7338.
Radda, G. K. (1975) *Methods Membr. Biol. 4*, 97–188.
Ruf, H., & Grell, E. (1981) *Mol. Biol., Biochem. Biophys. 31*, 333–376.
Seelig, J. (1970) *J. Am. Chem. Soc. 92*, 3881–3887.
Seelig, J. (1977) *Q. Rev. Biophys. 10*, 353–418.
Shinitzky, M., & Barenholz, Y. (1978) *Biochim. Biophys. Acta 515*, 367–394.
Sikaris, K. A., Thulborn, K. R., & Sawyer, W. H. (1981) *Chem. Phys. Lipids 29*, 23–36.
Sklar, L. A., Hudson, B. S., & Simoni, R. D. (1977) *Biochemistry 16*, 819–828.
Sklar, L. A., Miljanich, G. P., & Dratz, E. A. (1979) *Biochemistry 18*, 1707–1716.
Stümpel, J., Eibl, H. J., & Niksch, A. (1983) *Biochim. Biophys. Acta 727*, 246–254.
Sturtevant, J. M., Ho, C., & Reimann, A. (1979) *Proc. Natl. Acad. Sci. U.S.A. 76*, 2239–2243.
Tardieu, A., Luzatti, V., & Reman, F. C. (1973) *J. Mol. Biol. 75*, 711–733.
Teissie, J., & Tsong, T. Y. (1981) *Biochemistry 20*, 1548–1554.
Thulborn, K. R., & Sawyer, W. H. (1978) *Biochim. Biophys. Acta 511*, 125–140.
Tilley, L., Thulborn, K. R., & Sawyer, W. H. (1979) *J. Biol. Chem. 254*, 2592–2594.
Träuble, H. (1971) *Naturwissenschaften 58*, 277–284.
Tsong, T. Y. (1974) *Proc. Natl. Acad. Sci. U.S.A. 71*, 2684–2688.
Tsong, T. Y., & Kanehisa, M. J. (1977) *Biochemistry 16*, 2674–2680.
Tümmler, B., Maass, G., Vögtle, F., Sieger, H., Heimann, U., & Weber, E. (1979) *J. Am. Chem. Soc. 101*, 2588–2598.
Tümmler, B., Herrmann, U., Maass, G., & Eibl, H. (1984) *Biochemistry* (following paper in this issue).
Vincent, M., deForesta, B., Gallay, J., & Alfsen, A. (1982) *Biochemistry 21*, 708–716.
Waldmann, H., & Oblath, A. (1938) *Chem. Ber. 71*, 366–370.
Waldmann, H., & Stengl, R. (1950) *Chem. Ber. 83*, 167–170.
Watts, A., Marsh, D., & Knowles, P. F. (1978) *Biochemistry 17*, 1792–1801.
Weber, G. (1971) *J. Chem. Phys. 55*, 2399–2407.
Weber, G. (1981) *J. Phys. Chem. 85*, 949–953.
Wittebort, R. J., Schmidt, C. F., & Griffin, R. G. (1981) *Biochemistry 20*, 4223–4228.
Wittebort, R. J., Blume, A., Huang, T. H., DasGupta, S. K., & Griffin, R. G. (1982) *Biochemistry 21*, 3487–3502.
Yguerabide, J., & Foster, M. C. (1981) *Mol. Biol., Biochem. Biophys. 31*, 199–269.